

STUDIES OF THE HYDROLYSIS OF ALUMINUM ACTIVATED BY ADDITIONS OF Ga–In–Sn EUTECTIC ALLOY, BISMUTH, OR ANTIMONY

F. D. Manilevich,^{1,2} Yu. K. Pirskyy,¹ B. I. Danil'tsev,¹
A. V. Kutsyi,¹ and V. A. Yartys³

UDC 669.717:661.96

We study the Ga–In–Sn eutectic-catalyzed interaction of aluminum alloys with water resulting in the process of hydrolysis and generation of hydrogen. The aluminum alloys were prepared by melting aluminum with additions of Ga–In–Sn eutectic (5 wt.%), bismuth (3 wt.%), or antimony (3 wt.%). The temperature-dependent kinetics of their hydrolysis in a temperature range 25–70°C is studied by using a volumetric technique. The most efficient activation of the hydrolysis process is achieved for the Al–Ga–In–Sn alloy. The addition of bismuth to the Al–Ga–In–Sn alloy significantly decreases the hydrolysis rate, whereas the addition of antimony has only a weak effect on the process, despite the fact that the standard electrode potentials of bismuth and antimony have close values. The interactions of the studied alloys with water can be well fitted as a topochemical process. The modified Prout–Tompkins equation is used to get the effective hydrolysis-rate constants and it is shown that they increase following the temperature rise within the temperature range from 25 to 70°C. The activation energies of the process of hydrolysis for the studied alloys are calculated from the temperature dependence of the values of effective rate constants, which indicates that, within the main range of hydrogen generation (after the completion of the induction period and prior to the onset of deceleration of hydrogen release), the process of hydrolysis can be described as a diffusion-limited process.

Keywords: hydrolysis, aluminum alloys, hydrogen generation, Ga–In–Sn eutectic alloy, kinetics of hydrolysis.

Introduction

Hydrogen is an eco-friendly energy carrier with high energy content (122 MJ/kg). Moreover, as a chemical, it has valuable reducing properties and is broadly used in the chemical industry [1–3]. For the last decades, hydrogen-based power generation, which employs hydrogen both as an energy carrier and as a fuel has been rapidly developed [1–5]. In particular, the demand for fuel cells used for various purposes in which hydrogen fuel is converted into the electric current by using the anodic oxidation of hydrogen and the corresponding cathodic process has significantly increased. The development of autonomous power sources on the basis of fuel cells and hydrogen generators or H-stores solves the problem of powering a wide range of portable electric and electronic devices [1–7].

The expansion of application scopes and increase in the scale of used hydrogen call for improving the technologies of its production, transportation and storage. At present, the major part of hydrogen (80–90%) is produced from hydrocarbons, although their natural resources are running short [1, 8]. On the other hand, Earth's

¹ Vernadskii Institute of General and Inorganic Chemistry, Ukrainian National Academy of Sciences, Kiev, Ukraine.

² Corresponding author; e-mail: fedor@ionc.kar.net.

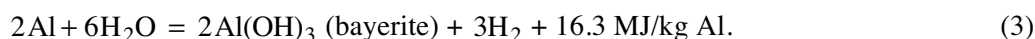
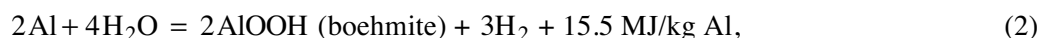
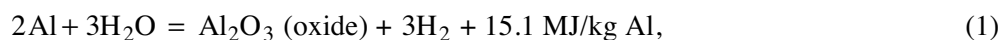
³ Institute for Energy Technology, Kjeller, Norway.

hydrosphere contains about $1.4 \cdot 10^{18}$ tons of water (H_2O) providing unlimited resources of hydrogen. The electrochemical decomposition of liquid water or water vapor is a well-developed and long-used method of hydrogen production [1, 9, 10]. However, the electrochemical production of hydrogen from water needs a significant amount of electrical energy to split water molecules. Numerous investigations aimed at improving and optimizing the electrolysis of water did not result in the reduction of the cost of hydrogen production [1, 3, 5–7, 9, 10]. The methods of water splitting based on the thermochemical cycles using the thermal energy ($\sim 800^\circ C$) of nuclear reactors or solar power plants are also applied [1, 11, 12]. The implementation of these methods requires complex engineering solutions and materials with high corrosion resistance. The photoelectrochemical water splitting performed by using semiconductor materials is also well developed [13–16]. The biochemical water splitting with the help of specially bred types of algae and microorganisms was also proposed [17, 18]. However, these methods have not yet found wide practical application, mainly due to their low efficiency and insufficient productivity.

Hydrogen generation performed by using water with various energy-storage substances (ESS) under variable conditions is of significant interest [19]. These conditions include chemical interactions between the ESS and the water-hydrolysis reaction. Hydrogen generation from water by using ESS is carried out in hydrolysis-type hydrogen generators [20]. These generators can be autonomous and portable. Moreover, they are convenient for the generation of hydrogen directly on site. Their application gives great benefits due to the elimination of significant problems connected with the accumulation, storage, and transportation of hydrogen.

To produce hydrogen by hydrolysis, it is possible to use binary and complex metal hydrides (MgH_2 , $NaBH_4$, $LiBH_4$, etc.) and individual metals that can react with water (Al, Mg, other low-melting point metals, and their alloys) [1, 19]. The hydrolysis of metal hydrides is accompanied by the evolution of much larger amounts of hydrogen than the hydrolysis of metals but hydrides are much more expensive than metals. Moreover, they are hygroscopic, susceptible to the action of atmospheric oxygen, and require storage in dry inert gases [21].

The aluminum-based ESS are promising for the release of hydrogen from water. As the advantages of aluminum in its application as ESS, we can mention its high energy capacity (31.1 MJ/kg) [2, 22], relatively low cost (~ 1.8 USD/kg), high availability, low density, convenient and safe transportation and storage, fairly large productivity in terms of the amount of hydrogen evolved in the course of hydrolysis, and the simplicity of hydrogen-generation systems. Depending on the conditions, there are three possible paths of the reaction of aluminum with water described by the following equations:



All three reactions are exothermic and, in all cases, the amount of hydrogen evolved from water is the same and equal to 1244 L/kg of Al or 111 g/kg of Al [23–25]. The aluminum products obtained in the process of hydrolysis are inert and eco-friendly substances that can be used to recuperate aluminum or to manufacture ceramics, absorbents, paper, fillers, etc. [1, 26–28].

Aluminum has a very negative value of the standard electrode potential ($E_{Al^{3+}/Al^0}^0 = -1.662$ V) [29] and, thus, readily and rapidly reacts with water in the absence of protective films. However, under normal conditions, the reaction of aluminum with water does not run because the aluminum surface is covered with a thin

oxide film. To activate aluminum, this dense film must be removed or cracked in order to expose the bare metal surface of aluminum.

There are various chemical, mechanochemical, and mechanical methods used for the activation of aluminum [22, 30]. Numerous studies [1, 8, 19–23, 25–28, 30–40] demonstrated that an effective way of activating aluminum and getting high rates of hydrogen generation from its reaction with water is to alloy aluminum with metals and nonmetals (Ga, Bi, Sn, In, Ca, Li, Zn, Mg, Ni, Co, Si, etc.). In numerous papers, it was shown that aluminum activated by alloying with low-melting metals is able to react with water already at room temperature [8, 22, 32, 33, 36, 37–40]. In the present study, aluminum is activated as a result of formation of its alloys with a eutectic gallium-indium-tin alloy and with bismuth or antimony. Thus, we study the regularities of hydrolysis of the obtained ESS.

The results of investigations of the thermophysical properties of eutectic Ga–In–Sn alloy are given in [41, 42]. According to the data of different authors, Ga, In and Sn form an eutectic containing the following mass fractions of the components: 66.0–67.0% Ga, 20.5–22.0% In, and 10.0–13.5% Sn. The melting point of these alloys is $10.7 \pm 0.3^\circ\text{C}$ [42]. In [22] it is shown that the eutectic Ga–In–Sn alloy crystallizes during its cooling at a temperature of 28°C lower than its melting point. Therefore, it can be assumed that aluminum activated in this alloy can interact with water at temperatures much lower than $10.7 \pm 0.3^\circ\text{C}$.

The structure of the alloys of aluminum with gallium, indium and tin, the distributions of doping elements in alloys, and the regularities of their interaction with water were studied in many works [22, 32, 33, 36, 37]. An alloy containing 50 wt.% Al, 34 wt.% Ga, 11 wt.% In, and 5 wt.% Sn was synthesized in [22]. It was found that, at room temperature, this alloy was partially liquid and reacted with distilled water with generation of gaseous hydrogen. The interaction of aluminum with water was facilitated due to the presence of liquid alloy phase creating a liquid window on the crystalline surface. The average yield of hydrogen was 83.8%. The product of aluminum oxidation was bayerite, the other present components of the alloy did not react with water. Moreover, an In_3Sn intermetallic compound was found in the products of hydrolysis. As a result of the analysis of kinetics performed in [22], it was found that the order of the reaction of aluminum with water was equal to 0.7, whereas the activation energy was as high as 43.8 kJ/mole.

The authors of [32] obtained alloys of aluminum with gallium (3.8 wt.%), indium (1.5 wt.%), and tin (0.7 wt.%). They were able to change the cooling rate of the melt and to get alloys with different crystallite sizes. By using the EDS analysis, they found aluminum crystallites containing gallium with the atomic ratio $\text{Al} : \text{Ga} \approx 60:1$ together with small amounts of indium and tin. Major amounts of indium and tin were concentrated on the surface of crystallites. Using DSC, the authors of [32] showed that the melting point of the Ga–In–Sn grain-boundary phases is higher (by several degrees) and the temperature of their crystallization is lower than the melting point of the eutectic Ga–In–Sn alloy by several tens of degrees. The rate of interaction of these alloys with water increases as the crystallite size decreases and as temperature increases from 30 to 60°C . After immersion in water, solid samples of the alloys cracked within several seconds and formed powders. The reaction of fine-grained samples with water proceeds rapidly and almost up to the full completion, whereas the coarse-grained samples react with water at a lower rate and the process of hydrolysis is incomplete.

The kinetics of interaction between the investigated alloys and water was determined by using the following standard equation [32]:

$$\frac{d\alpha}{d\tau} = k(1 - \alpha)^n, \quad (4)$$

where α is a degree of conversion of aluminum; τ is the duration of reaction; k is the reaction rate constant, and n is the reaction order for aluminum. The computed values of the reaction order lied between 0.64 and 0.72, and the activation energies decreased from 77 ± 8 to 53 ± 4 kJ/mole following the decrease in crystallite

sizes from 258 to 23 μm . According to [32], the Ga–In–Sn liquid alloy introduced into aluminum not only protects aluminum against oxidation but also provides a path for the diffusion of its nanoparticles toward the site of interaction with water. Furthermore, since aluminum reacts with water on its bare surface, the aluminum hydroxide formed as a result of interaction between aluminum and water may partially block the surface of Al alloy and retard the process. However, due to the vigorous evolution of hydrogen, no dense hydroxide layer was formed on the alloy surface. The authors of [32] explained the fact that the reaction order for aluminum is less than 1 by the interaction of aluminum with water both on the bare crystalline surface partially blocked by aluminum hydroxide and in the spots covered with Ga–In–Sn alloy after diffusion through this alloy.

To study the effect of microstructure and phase composition of Al–Ga–In–Sn alloy on the regularities of its interaction with water, the ribbons 40–60 μm in thickness were made from the ingots of alloy that were annealed within a temperature range 250–500°C [36]. In the obtained ribbons, the authors identified the phase of solid solution of gallium in aluminum and the In_3Sn intermetallic phase. The increase in the annealing temperature from 300 to 500°C leads to an increase in the size of aluminum crystallites and particles of Ga–In–Sn alloy on their surface with decrease in the amount of particles of the ternary alloy. The studies of the interaction between the obtained activated aluminum ribbons and water at 30–60°C show that the decrease in the size of aluminum crystallite from 260 to 23 μm lead to an increase in the rate of hydrogen evolution. Moreover, as the crystallite size decreases further down to 3 μm , the rate of hydrogen evolution decreases to about 80% of its maximum value.

The effect of composition of the Ga–In–Sn alloy on the activity of aluminum in the reaction with water was studied in [37] by investigating a series of aluminum-based alloys with constant total content of gallium, indium and tin (6 wt.%) but with variations of their ratio. These alloys interact with water at temperatures as low as 0.5°C. However, within the temperature range 0.5–15°C, the interaction rate is unstable. A stable increase in the rate of hydrolysis of aluminum was reached when the temperature became higher than 15°C. At 50°C, the solid samples of alloys cracked after the immersion in water and turned into powders within dozens of seconds. The dependence of the rate of hydrogen generation at 50°C on the gallium content has a maximum for a gallium content of 3.8 wt.%. As a result of XRD investigations, it is possible to conclude that, for the indium-to-tin ratio equal to 15 : 7, the analyzed alloys contain a solid solution of gallium in aluminum and the In_3Sn intermetallic phase [37]. As the tin content increases up to the ratio $\text{In} : \text{Sn} = 1 : 1$, we also identify an InSn_4 intermetallic phase. The indicated increase in the tin content of the investigated alloys leads to a significant (~ 50%) increase in rate of hydrogen generation, which can be explained by the formation of aluminum-tin microgalvanic couples. In this case, aluminum undergoes anodic dissolution, and the cathodic hydrogen evolution from water takes place on the tin-rich particles.

The Al–Ga–Sn (1.73 wt.% Ga, 1 wt.% Sn) and Al–Ga–In (1.73 wt.% Ga, 1 wt.% In) alloys were obtained and investigated in [33]. At 30°C, the highest hydrogen evolution rate was attained in the course of hydrolysis of the Al–Ga–Sn alloy and the lowest rate was observed in the course of hydrolysis of the Al–Ga–In alloy. It is concluded that the rate of interaction between the alloys and water is determined by the difference between the electrode potentials of aluminum and added metals. Based on the theory of microgalvanic couples, the potential differences were calculated for the Al–Sn, Al–In, and Al–Ga couples. Thus, the largest differences were observed for the Al–Sn couple (– 1.53 V) and the smallest for the Al–Ga couple (– 1.15 V), i.e., the potential differences decreased in the following order: Al–Sn > Al–In > Al–Ga, which corresponded to the sequence of decrease in the aluminum dissolution rates in the interaction of the studied alloys with water [33].

The activation effect of the metals more electropositive than aluminum introduced into aluminum on its corrosion dissolution was considered in numerous reference works [34, 43–45]. As a result of the formation of microgalvanic couples, the potential of aluminum shifts to the negative values, which causes its rapid dissolution. The three-step mechanism of activation of the aluminum anodes proposed in [43] envisages the dissolution of aluminum occurring after the immersion of the alloy in a solution of electrolyte (step 1):

STEP 1.



Then the cations of more electropositive metal are reduced as a result of electron exchange with aluminum and the metal forms deposits on the aluminum surface (step 2):

STEP 2.



Step 3 occurs simultaneously with step 2 and can be described as the local detachment of the protective oxide film formed on the aluminum surface caused by the presence of a more electropositive metal on its surface:

STEP 3. Local detachment of the protective oxide film.

As a result, the aluminum surface becomes locally free of protective films and the potential of aluminum shifts to more negative values. Similar mechanisms were also proposed in [8, 34].

As both aluminum and gallium belong to the IIIA subgroup of the periodic table, they can readily form solid solutions [8]. Gallium and aluminum have close values of atomic radii (1.41 Å and 1.43 Å, respectively). Therefore, gallium can be dissolved in aluminum without significant distortions of the aluminum lattice. Indeed, according to the phase diagram of the Al–Ga system, the solubility of Ga in Al is 20 wt.% [34].

Indium is difficultly soluble in aluminum. According to the phase diagram of the Al–In system, its solubility in Al is 0.01–0.05 wt.% [34]. The introduction of indium into aluminum in the amounts exceeding its solubility limit results in the crystallization of indium on the surface of aluminum crystallites as an individual phase. Tin also has a low solubility in aluminum and forms intermetallic compounds with indium (in the presence of In in the alloy) appearing on the aluminum surface. The composition of In–Sn intermetallic compounds depends on the In : Sn ratio in the alloy. As an example, in the alloy containing 97 wt.% Al, 1.75 wt.% Ga, indium, and tin, the only intermetallic compound formed for a tin content of < 0.35 wt.% is β -In₃Sn [35]. The increase in the tin content from 0.35 to 0.9 wt.% leads to an increase in the γ -InSn₄ content and a decrease in the β -In₃Sn content. In the presence of > 0.9 wt.% of tin, the only detected phase was γ -InSn₄. The particles of In–Sn intermetallics formed on the surfaces of the aluminum crystallites create microgalvanic couples with aluminum, which facilitates its dissolution. The authors of [35] also found that the dependence of the rate of H₂ generation by the interaction of Al–Ga–In–Sn alloy with water on the content of tin within the temperature range 60–75°C has a maximum for a tin content of 0.5 wt.%, which corresponds to the maximum amount of the β -In₃Sn phase present on the surfaces of Al crystallites.

Thus, the temperature at which the aluminum-based ESS react with water, reaction rate, and hydrogen yield depend on the nature of added metals-activators, their contents in the ESS, and the conditions of alloy preparation. It should be also noted that the duration of storage and the conditions of ESS based on aluminum activated with liquid metals and alloys are important for the extent of their activity and hydrogen yield during their interaction with water. According to the results obtained in [31], the alloy of aluminum (80 wt.%) with gallium, indium, tin, and zinc retained its activity only after storage at the temperature of liquid nitrogen. As a result of storage of alloys in a vacuum, in inert atmospheres, and (especially) in air, the hydrogen yield caused by the interaction of these alloys with water decreases. However, in [37] it was shown that bulk samples of activated aluminum retain their activity for at least one month in the case of storage in dry air with a humidity of less than 20%. Therefore, for the long-term storage of aluminum-based ESS, it is important to seal them in plastic bags filled with inert gases.

The Ga–In–Sn eutectic alloy introduced into aluminum exerts a noticeable influence as a catalyst in the reaction of aluminum with water, since the components of alloy accelerate the dissolution of aluminum but do not react with water [22]. The amount of the eutectic Ga–In–Sn alloy used to activate aluminum must be greater than the minimum value required to get the desired rate of hydrogen generation at a given temperature. It was shown that aluminum activated with the Ga–In–Sn eutectics generates hydrogen from water at 25°C if the content of this alloy is ≥ 3 wt.% [46]. However, the activity of these aluminum-based ESS can decrease with time. This is why, in this study, the amount of eutectic Ga–In–Sn alloy introduced into aluminum was equal to 5 wt.%. Furthermore, to investigate the effect of electropositive additives on the regularities of interaction between activated aluminum and water, additions of bismuth or antimony (3 wt.% each) were introduced into the studied alloys.

Experimental

To prepare aluminum-based ESS, we used high-purity metals (≥ 99.9 wt.%). The eutectic Ga–In–Sn alloy with mass fractions of the components of 67/22/11% was prepared by adding the required weighted amounts of indium powder and tin to molten gallium kept at 50°C. The mixture was held at 50°C for 30 min with periodic stirring. After cooling down to room temperature the obtained alloy remained in the liquid state.

Aluminum with appropriate additions of eutectic Ga–In–Sn alloy and Bi or Sb was melted in an electric shaft furnace in an argon atmosphere with mechanical stirring. The computed amount of aluminum was placed in an alundum crucible inserted in an electric furnace. The crucible was covered with a quartz cover with holes for feeding argon and mounting an alundum stirrer. Argon was delivered in the crucible through a quartz tube. The aluminum was melted at 900°C and the computed amounts of the preliminarily prepared eutectic Ga–In–Sn alloy and Bi or Sb were added to the molten metal. After this, the melt was stirred for 30 min with an alundum blade stirrer connected to an electric motor. The melt was quickly poured into a flat rectangular graphite mold. The thickness of the melted layer in the mold was smaller than 5 mm, which ensured high rates of its cooling. After cooling, the obtained alloys were sealed in double polyethylene bags filled with high-purity argon.

The regularities of hydrogen evolution during interaction between the obtained ESS and water were studied by measuring the volume of evolved hydrogen. A setup for volumetric measurements consisted of a thermostated beaker, a connecting tube, and a eudiometer. Distilled water (100 mliter) was poured in the beaker, which was preliminarily saturated with hydrogen. After this, an alloy sample with a mass of 1 g in the form of a rectangular parallelepiped was placed into water. The beaker was hermetically sealed. Hydrogen evolving in the course of hydrolysis of aluminum entered the eudiometer where its volume was measured at regular intervals. The water temperature was kept constant by using a U-4 thermostat.

The average rate of hydrogen evolution for the time of interaction between the alloys and water is given by the formula

$$v = \frac{V_0}{\tau}, \quad (7)$$

where V_0 is the volume of H_2 (under normal conditions) evolved for time τ .

The volume of evolved hydrogen was converted to the normal conditions ($T = 273.15^\circ\text{K}$ and a pressure of 760 mm Hg) according to the formula:

$$V_0 = \frac{273.15 V_\tau \left(P - p - \frac{h_{H_2O}}{13.6} \right)}{760(273.15 + t)}, \quad (8)$$

where V_t is the volume of hydrogen measured at room temperature t ($^{\circ}\text{C}$) and the barometric pressure P (mm-Hg); p is a pressure of water vapor (mm-Hg) at the same temperature; $h_{\text{H}_2\text{O}}$ is the height of water column in the eudiometer (mm), and 13.6 is the density of mercury (g/cm^3).

Results and Discussion

Bismuth and antimony have positive values of standard electrode potentials ($E_{\text{Bi}^{3+}/\text{Bi}^0}^{\circ} = 0.20 \text{ V}$ and $E_{\text{Sb}^{3+}/\text{Sb}^0}^{\circ} = 0.24 \text{ V}$ [29]). They were chosen as additives to aluminum activated with the Ga–In–Sn eutectic alloy. The difference between the standard electrode potentials of aluminum and bismuth is -1.862 V ; and, for the difference between aluminum and antimony, we have -1.902 V . The obtained and investigated aluminum-based alloys contain 5 wt.% eutectic Ga–In–Sn alloy and 3.0 wt.% Bi (or Sb).

As follows from Fig. 1, the introduction of bismuth into aluminum activated by the Ga–In–Sn eutectic leads to a significant decrease in H_2 generation rate. However, the introduction of antimony into the activated aluminum only slightly affects the regularities of hydrogen evolution: they are close to the regularities of hydrogen evolution in the course of hydrolysis of aluminum activated solely by the Ga–In–Sn eutectic.

At the beginning of interaction between the investigated ESS and water, we observe a sharp increase in the rate of hydrogen evolution as a result of the activation and growth of the reacting aluminum surface, especially when the samples are cracked and disintegrated. However, after the consumption of the main amount of aluminum, the rate of hydrogen accumulation decreases and, hence, the plots of v vs. τ contain maxima. The samples of activated aluminum with additions of bismuth did not crack during hydrolysis. Therefore, after the completion of the period of activation of their surface, the v – τ plots showed only a mostly constant rate of hydrogen generation, which is important for simplification of the system of hydrogen supply of fuel cells.

Thus, the effects of bismuth and antimony on the activity of aluminum are strongly different, despite the fact that bismuth and antimony have close values of the standard electrode potential. The electrochemical properties of these additives do not apparently determine their effects on the regularities of interaction between Al and water. However, the process of formation of the alloy modified by additives and their ability to form intermetallics with the other components of the investigated ESS are of crucial importance, which calls for the additional studies.

Raising the temperature of hydrolysis of all alloys from 25 to 70°C leads to a significant increase in the volume of evolved hydrogen and a decrease in the duration of their hydrolysis (see Fig. 2). It should be noted that the sigmoidal shape of the obtained V_0 – τ plots containing a bend is typical of the topochemical reactions, i.e., heterochemical reactions running for the solids [47, 48].

Hydrogen yield sharply increases with temperature, and the time of attainment of its maximum values significantly decreases. As an example, in the process of hydrolysis of the Al–Ga–In–Sn alloy carried out at a temperature of 25°C for 320 min, we observe the evolution only of 19.5% from the theoretically possible amount of hydrogen. At the same time, at 70°C , the hydrogen yield was as high as 98.8% after 23 min. The Al–Ga–In–Sn–Bi alloy was less active, and the hydrogen yield in the course of its hydrolysis for 450 min at 25°C was as low as 3.5%. However, the process of hydrolysis at 70°C for 120 min resulted in a hydrogen yield of 99.3%. For the Al–Ga–In–Sn–Sb alloy, hydrogen yield observed as a result of hydrolysis at 25°C for 420 min is equal to 20.7%. At the same time, after 70 min at 70°C , it becomes as high as 99.7%.

Most v – τ plots have maxima that are reached faster and become higher as the temperature of hydrolysis increases (see Fig. 3). As the temperature increases from 25 to 70°C , we observe a significant increase in the maximum rate of hydrogen generation in the process of hydrolysis for all investigated alloys.

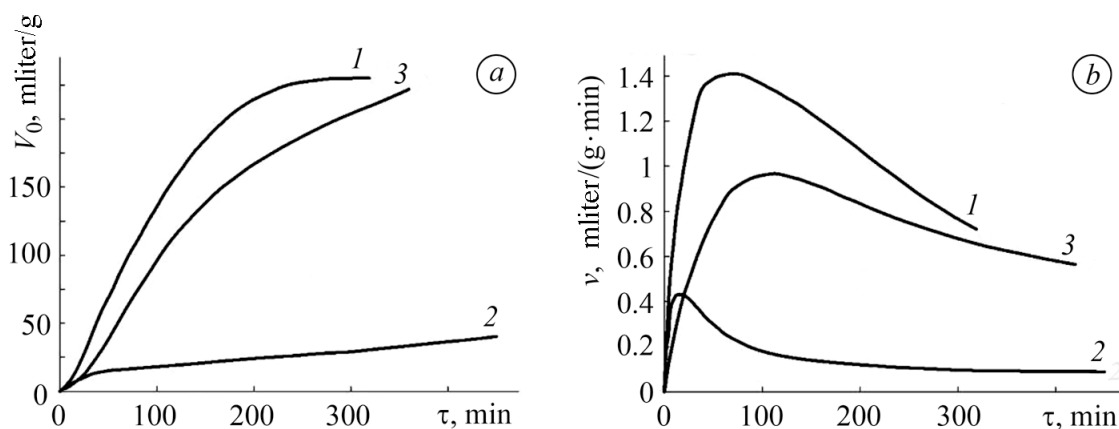


Fig. 1. Time dependences of the volume of generated hydrogen (a) and the average rate of its evolution (b) during hydrolysis of aluminum activated by the Ga-In-Sn eutectic alloy (5 wt.%) (1) and bismuth (3 wt.%) (2) or antimony (3 wt.%) (3) measured at 25°C.

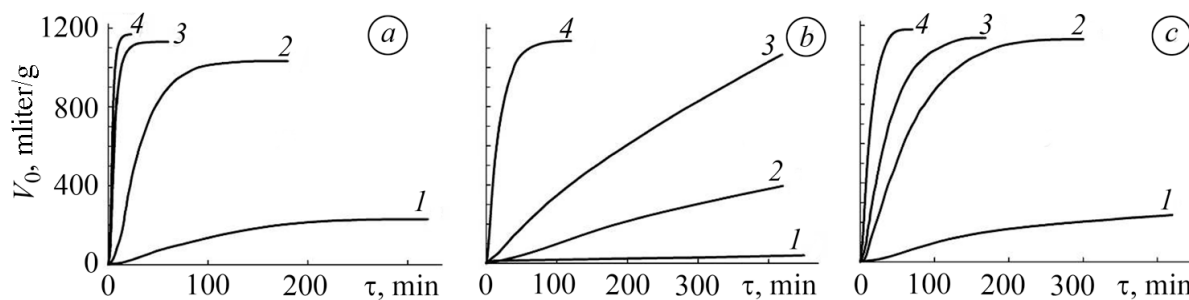


Fig. 2. Time dependences of the volume of hydrogen evolved in the course of hydrolysis of aluminum activated with the Ga-In-Sn eutectic alloy (a) and bismuth (b) or antimony (c) at the following temperatures (°C): 25 (1); 40 (2); 55 (3); 70 (4).

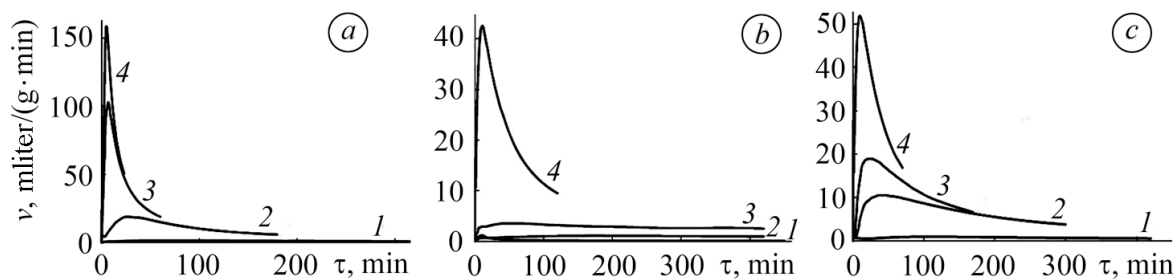


Fig. 3. Average rates of hydrogen evolution in the course of hydrolysis of aluminum activated with the eutectic Ga-In-Sn alloy (a) and bismuth (b) or antimony (c) versus the time of hydrolysis at the following temperatures (°C): 25 (1); 40 (2); 55 (3); 70 (4).

In particular, in the process of hydrolysis of aluminum activated solely with the Ga-In-Sn eutectic, the maximum value of v increases by two orders of magnitude (from 1.42 to 158.6 mliter/(g·min)). A large plateau can be seen in the v - τ plots during the hydrolysis of activated aluminum with additions of bismuth at 25–55°C when hydrogen is generated at an almost constant rate.

To determine the effective rate constants (k^e) of the reactions of hydrolysis of aluminum accompanying the interaction between the aluminum-based ESS and water, we used the Prout-Tompkins equation that describes

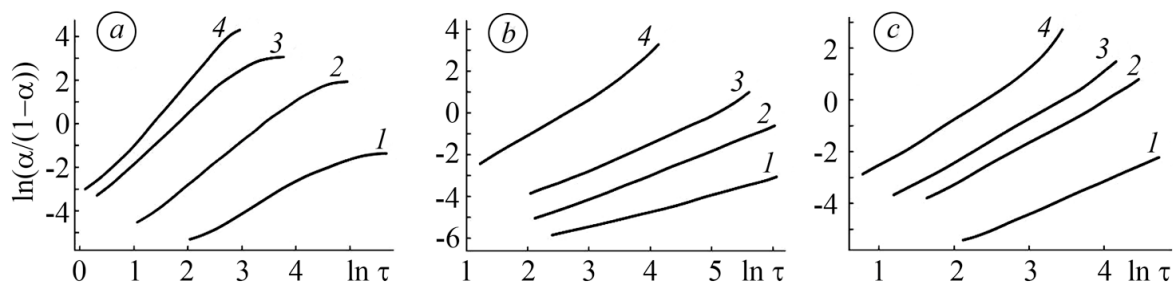


Fig. 4. The dependences of $\ln[\alpha/(1-\alpha)]$ on $\ln \tau$ plotted in the process of hydrolysis of aluminum activated with the Ga–In–Sn eutectic alloy (a) and bismuth (b) or antimony (c) at the following temperatures ($^{\circ}\text{C}$): 25 (1); 40 (2); 55 (3); 70 (4).

the topochemical reactions of decomposition of solid materials through the crystalline cracking running on the boundary between these materials and the solid products of decomposition [47–49]:

$$\ln \left[\frac{1}{1-\alpha} \right] = k^e \tau + C, \quad (9)$$

where C is an integration constant. In the differential form, Eq. (9) looks like:

$$\frac{d\alpha}{dt} = k^e \alpha(1-\alpha). \quad (10)$$

This implies that the reaction rate depends both on the amount of the reacting substance and on the amount of the product. These reactions belong to the autocatalytic processes [49].

The degree of conversion of aluminum was computed as the ratio of the volume of evolved hydrogen to the theoretical value corresponding to the case where the reaction of hydrolysis is complete. The clearly developed linear sections are not present in the plots of $\ln[\alpha/(1-\alpha)]$ on τ . Hence, it is necessary to apply the modified Prout–Tompkins equation presenting the inverse variation of the effective rate constant of the topochemical reaction as a function of time [49], namely,

$$\ln \left[\frac{\alpha}{1-\alpha} \right] = k^e \ln \tau + C. \quad (11)$$

All obtained $\ln[\alpha/(1-\alpha)]-\ln \tau$ dependences (see Fig. 4) contain an induction period of interaction, which is common for the topochemical reactions [47, 48]. At the end of the induction period, these dependences reveal the presence of prolonged linear sections. Finally, at the end of the linear intervals, the curves show the onset of the retardation process.

The values of the effective rate constants of interaction between aluminum and water are determined as the slopes of the linear sections of the plots shown in Fig. 4 (see Table 1). The highest values of k^e are observed in the course of hydrolysis of activated aluminum without Bi or Sb additives. As temperature increases from 25 to 70 $^{\circ}\text{C}$, the values of k^e increase for all studied ESS.

The temperature dependences of the effective rate constants of hydrolysis for the investigated ESS were used to calculate the activation energies of this process according to the Arrhenius equation (Table 1). The obtained values of the activation energy are low and indicate that the hydrolysis of the investigated aluminum-based ESS proceeds as a diffusion-controlled process that starts at the end of the induction period and terminates prior to the development of the process of deceleration.

Table 1
Effective Rate Constants and Activation Energies for the Hydrolysis of Aluminum Activated with the Ga–In–Sn Eutectic Alloy and Bi or Sb at Various Temperatures

Alloy	Temperature (°C)				E_a , kJ/mole
	25	40	55	70	
	k^e , min ⁻¹				
Al + 5 wt.% Ga–In–Sn	1.46	1.98	2.33	2.90	12.60
Al + 5 wt.% Ga–In–Sn + 3 wt.% Bi	0.81	1.17	1.34	1.73	13.75
Al + 5 wt.% Ga–In–Sn + 3 wt.% Sb	1.27	1.58	1.69	1.88	7.10

CONCLUSIONS

The activation of aluminum by the addition of the Ga–In–Sn eutectic alloy, bismuth, or antimony dramatically improves the performance of the individual Al metal used in the process of hydrolysis in order to generate gaseous hydrogen as a result of interaction with water at temperatures higher than 25°C. The most efficient performance in the reaction of hydrolysis is achieved for aluminum doped only with the Ga–In–Sn eutectic (5 wt.%). Bulk samples of this alloy suffer cracking and become decrepitated when interacting with water in the process of hydrolysis. It appears that the additives of bismuth and antimony differently affect the regularities of hydrolysis of activated aluminum despite the close values of their standard electrode potentials. Indeed, while additions of bismuth (3 wt.%) to the Al–Ga–In–Sn alloy significantly decrease the rate of hydrolysis, the additions of antimony (3 wt.%) lead only to a slight decrease in the rate of hydrolysis. However, within the temperature range 25–55°C, an almost constant rate of hydrogen generation can be achieved for a long period of time for the Al–Ga–In–Sn alloy doped with 3 wt.% Bi. The indicated slower interaction is not accompanied by cracking and powdering of the samples of bulk alloy.

The kinetics of the process of hydrogen generation is described by sigmoidal plots of the time dependence of the volume of generated hydrogen indicating that the reactions of the investigated alloys with water are topochemical processes. The values of the effective rate constants of the hydrolysis for all studied alloys are determined using the modified Prout–Tompkins equation and show an increase when the temperature is rising from 25 to 70°C. The values of activation energy of the process of hydrolysis calculated from the temperature dependence of the effective rate constants indicate that the hydrolysis is a diffusion-controlled process, which includes, in addition to the period of intense H₂ generation, the induction period and the step of retardation of the interaction of alloy with water.

Acknowledgements. The present work was supported by the NATO SPS program (Project G5233 Portable Energy Supply). The authors are grateful to Prof. I. Yu. Zavalij for his kind help.

REFERENCES

1. L. F. Kozin and S. V. Volkov, *Contemporary energetics and Ecology: Problems and Prospects* [in Russian], Naukova Dumka, Kiev (2006).
2. R. Ramachandran and R. K. Menon, "An overview of industrial uses of hydrogen," *Int. J. Hydrogen Energy*, **23**, No. 7, 593–598 (1998).

3. C.-J. Winter, "Hydrogen energy—Abundant, efficient, clean: A debate over the energy-system-of-change," *Int. J. Hydrogen Energy*, **34**, No. 14, S1–S52 (1998).
4. B. P. Tarasov and M. V. Lototskiy, "Hydrogen energetics: past, present, and prospects," *Russ. Khim. Zh.*, **50**, No. 6, C. 5–18 (2006).
5. V. A. Goltsov, T. N. Veziroglu, and L. F. Goltsova, "Hydrogen civilization of the future—A new conception of the IAHE," *Int. J. Hydrogen Energy*, **31**, No. 2, 153–159 (2006).
6. O. Gröger, H. A. Gasteiger, and J.-P. Suchsland, "Review—Electromobility: Batteries or Fuel Cells?," *J. Electrochem. Soc.*, **162**, No. 14, A2605–A2622 (2015).
7. R. O'Hayre, S.-W. Cha, W. Colella, and F. B. Prinz, *Fuel Cell Fundamentals*, John Wiley & Sons, Hoboken, NJ (2016).
8. S. Hu, X. Zhao, and J. Liu, "Liquid metal activated aluminum-water reaction for direct hydrogen generation at room temperature," *Renew. Sustain. Energy Reviews*, **92**, 17–37 (2018).
9. T. E. Lipman and A. Z. Weber (editors), *Fuel Cells and Hydrogen Production*, Springer, NY (2019).
10. D. Lj. Stojić, M. P. Marčeta, S. P. Sovilj, and Šć. S. Miljanić, "Hydrogen generation from water electrolysis—possibilities of energy saving," *J. Power Sources*, **118**, No. 1–2, 315–319 (2003).
11. M. F. Orhan, I. Dincer, M. A. Rosen, and M. Kanoglu, "Integrated hydrogen production options based on renewable and nuclear energy sources," *Renew. Sustain. Energy Reviews*, **16**, No. 8, 6059–6082 (2012).
12. B. Yildiz and M. S. Kazimi, "Efficiency of hydrogen production systems using alternative nuclear energy technologies," *Int. J. Hydrogen Energy*, **31**, No. 1, 77–92 (2006).
13. D. Kandi, S. Martha, and K. M. Parida, "Quantum dots as enhancer in photocatalytic hydrogen evolution: A review," *Int. J. Hydrogen Energy*, **42**, No. 15, 9467–9481 (2017).
14. P. Sharma and M. L. Kolhe, "Review of sustainable solar hydrogen production using photon fuel on artificial leaf," *Int. J. Hydrogen Energy*, **42**, No. 36, 22704–22712 (2017).
15. F. Yilmaz, M. T. Balta, and R. Selbaş, "A review of solar based hydrogen production methods," *Renew. Sustain. Energy Reviews*, **56**, 171–178 (2016).
16. H. Ahmad, S. K., Kamarudin L. J. Minggu, and M. Kassim, "Hydrogen from photo-catalytic water splitting process: A review," *Renew. Sustain. Energy Reviews*, **43**, 599–610 (2015).
17. A. Tanksale, J. N. Beltramini, and G. M. Lu, "A review of catalytic hydrogen production processes from biomass," *Renew. Sustain. Energy Reviews*, **14**, No. 1, 166–182 (2010).
18. L. Guo, X. M. Li, G. M. Zeng, and Y. Zhou, "Effective hydrogen production using waste sludge and its filtrate," *Energy*, **35**, No. 9, 3557–3562 (2010).
19. I. L. Varshavskiy, *Energy-Accumulating Substances and Their Applications* [in Russian], Naukova Dumka, Kiev (1980).
20. R. S. Nazarov, S. D. Kushch, O. V. Kravchenko, É. É. Fokina, and B. P. Tarasov, "Hydrogen-generating materials for the sources of hydrogen of the hydrolysis type," *Alternative Energetics and Ecology*, No. 6(86), 26–32 (2010).
21. L. Soler, J. Macanás, M. Muñoz, and J. Casado, "Aluminum and aluminum alloys as sources of hydrogen for fuel cell applications," *J. Power Sources*, **169**, No. 1, 144–149 (2007).
22. J. T. Ziebarth, J. M. Woodall, R. A. Kramer, and G. Choi, "Liquid phase-enabled reaction of Al–Ga and Al–Ga–In–Sn alloys with water," *Int. J. Hydrogen Energy*, **36**, No. 9, 5271–5279 (2011).
23. A. V. Parmuzina and O. V. Kravchenko, "Activation of aluminum metal to evolve hydrogen from water," *Int. J. Hydrogen Energy*, **33**, No. 12, 3073–3076 (2008).
24. G. N. Ambaryan, M. S. Vlaskin, A. O. Dudoladov, E. A. Meshkov, A. Z. Zhuk, and E. I. Shkolnikov, "Hydrogen generation by oxidation of coarse aluminum in low content alkali aqueous solution under intensive mixing," *Int. J. Hydrogen Energy*, **41**, No. 39, 17216–17224 (2016).
25. V. Rosenband and A. Gany, "Application of activated aluminum powder for generation of hydrogen from water," *Int. J. Hydrogen Energy*, **35**, No. 20, 10898–10904 (2010).
26. A. V. Ilyukhina, A. S. Ilyukhin, and E. I. Shkolnikov, "Hydrogen generation from water by means of activated aluminum," *Int. J. Hydrogen Energy*, **37**, No. 21, 16382–16387 (2012).
27. A. Babak and M. Korosh, "A novel method for generating hydrogen by hydrolysis of highly activated aluminum nanoparticles in pure water," *Int. J. Hydrogen Energy*, **34**, No. 19, 7934–7938 (2009).
28. M. Korosh and A. Babak, "Enhancement of hydrogen generation in reaction of aluminum with water," *Int. J. Hydrogen Energy*, **35**, No. 11, 5227–5232 (2010).
29. G. Milazzo and S. Caroli, *Tables of Standard Electrode Potentials*, Wiley, NY (1978).
30. E. I. Shkolnikov, A. Z. Zhuk, and M. S. Vlaskin, "Aluminum as energy carrier: Feasibility analysis and current technologies overview," *Renewable and Sustainable Energy Reviews*, **15**, No. 9, 4611–4623 (2011).
31. O. V. Kravchenko, K. N. Semenenko, B. M. Bulychev, and K. B. Kalmykov, "Activation of aluminum metal and its reaction with water," *J. Alloys Comp.*, **397**, No. 1–2, 5227–5232 (2005).
32. W. Wang, D. M. Chen, and K. Yang, "Investigation on microstructure and hydrogen generation performance of Al-rich alloys," *Int. J. Hydrogen Energy*, **35**, No. 21, 12011–12019 (2010).
33. T. He, W. Wang, W. Chen, W. Chen, D. Chen, and K. Yang, "Reactivity of Al-rich alloys with water promoted by liquid Al grain boundary phases," *J. Mat. Sci. Tech.*, **33**, No. 4, 397–403 (2017).

34. C. Ying, L. Bei, W. Huihu, and D. Shijie, “Effects of preparation parameters and alloy elements on the hydrogen generation performance of aluminum alloy – 0°C pure water reaction,” *Rare Metal Mater. Eng.*, **46**, No. 9, 2428–2432 (2017).
35. T. T. He, W. Wang, W. Chen, D. M. Chen, and K. Yang, “Influence of In and Sn compositions on the reactivity of Al–Ga–In–Sn alloys with water,” *Int. J. Hydrogen Energy*, **42**, No. 9, 5627–5637 (2017).
36. W. Wang, X. M. Zhao, D. M. Chen, and K. Yang, “Insight into the reactivity of Al–Ga–In–Sn alloy with water,” *Int. J. Hydrogen Energy*, **37**, No. 3, 2187–2194 (2012).
37. W. Wang, W. Chen, X. M. Zhao, D. M. Chen, and K. Yang, “Effect of composition on the reactivity of Al-rich alloys with water,” *Int. J. Hydrogen Energy*, **37**, No. 24, 18672–18678 (2012).
38. C. C. Wang, Y. C. Chou, and C. Y. Yen, “Hydrogen generation from aluminum and aluminum alloys powder,” *Proc. Eng.*, **36**, 105–113 (2012).
39. H. Z. Wang, D. Y. C. Leung, M. K. H. Leung, and M. Ni, “A review on hydrogen production using aluminum and aluminum alloys,” *Renewable and Sustainable Energy Reviews*, **13**, No. 4, 845–853 (2009).
40. M. Q. Fan, F. Xu, and L. X. Sun, “Studies on hydrogen generation characteristics of hydrolysis of the ball milling Al-based materials in pure water,” *Int. J. Hydrogen Energy*, **32**, No. 14, 2809–2815 (2007).
41. D. S. Evans and A. Prince, “Thermal analysis of Ga–In–Sn system,” *Metal Sci.*, **12**, No. 9, 411–414 (1978).
42. Yu. Plevachuk, V. Sklyarchuk, Sv. Eckert, G. Gerbeth, and R. Novakovic, “Thermophysical properties of the liquid Ga–In–Sn eutectic alloy,” *J. Chem. Eng. Data*, **59**, No. 3, 757–763 (2014).
43. M. C. Reboul, Ph. Gimenez, and J. J. Rameau, “A proposed activation mechanism for Al anodes,” *Corrosion*, **40**, No. 7, 366–371 (1984).
44. C. B. Breslin and W. M. Carroll, “The electrochemical behavior of aluminum activated by gallium in aqueous electrolytes,” *Corr. Sci.*, **33**, No. 11, 1735–1746 (1992).
45. A. Venugopal and V. S. Raja, “AC impedance study on the activation mechanism of aluminum by indium and zinc in 3.5% NaCl medium,” *Corr. Sci.*, **39**, No. 12, 2053–2065 (1997).
46. F. D. Manilevich, L. Kh. Kozin, B. I. Danil’tsev, A. V. Kutsyi, and Yu. K. Pirskeyy, “Regularities of the hydrolysis of aluminum activated with the eutectic alloy of gallium, indium, and tin,” *Ukr. Khim. Zh.*, **83**, No. 7, C. 51–59 (2017).
47. B. Delmont, *Kinetics of Heterogeneous Reactions* [Russian translation], Mir, Moscow (1972).
48. P. Barre, *Kinetics of Heterogeneous Processes* [Russian translation], Mir, Moscow (1976).
49. M. E. Brown, “The Prout–Tompkins rate equation in solid-state kinetics,” *Thermochim. Acta*, **300**, No. 1–2, 93–106 (1997).